Science of the Total Environment xxx (xxxx) xxx

Contents lists available at ScienceDirect

Science of the Total Environment

journal homepage: www.elsevier.com/locate/scitotenv

Influenza seasonality and its environmental driving factors in mainland China and Hong Kong

Sheikh Taslim Ali [a,b], Benjamin J. Cowling [a,b,*], Jessica Y. Wong [a], Dongxuan Chen [a,b], Songwei Shan [a,b], Eric H.Y. Lau [a,b], Daihai He [c], Linwei Tian [a], Zhongjie Li [d], Peng Wu [a,b]

[a] *WHO Collaborating Centre for Infectious Disease Epidemiology and Control, School of Public Health, Li Ka Shing Faculty of Medicine, The University of Hong Kong, Hong Kong Special Administrative Region*
[b] *Laboratory of Data Discovery for Health, Hong Kong Science and Technology Park, Hong Kong Special Administrative Region*
[c] *Department of Applied Mathematics, Hong Kong Polytechnic University, Hong Kong Special Administrative Region*
[d] *Chinese Center for Disease Control and Prevention, Beijing, China*

HIGHLIGHTS

- U-shaped association between ambient absolute humidity and influenza transmissibility
- Interpreting single winter peak in temperate and both summer and winter peaks in tropics
- Absolute humidity, a stronger predictor can explain up to 15% of variance in transmissibility.

GRAPHICAL ABSTRACT

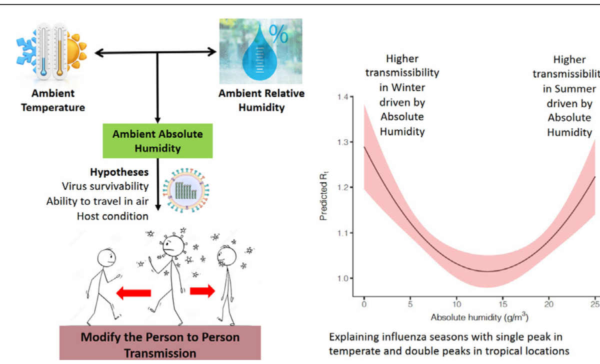

ARTICLE INFO

Article history:
Received 19 August 2021
Received in revised form 20 October 2021
Accepted 12 November 2021
Available online xxxx

Editor: SCOTT SHERIDAN

Keywords:
Influenza virus
Transmissibility
Seasonality
Prediction
Humidity

ABSTRACT

Background: Influenza epidemics occur during winter in temperate zones, but have less regular seasonality in the subtropics and tropics. Here we quantified the role of environmental drivers of influenza seasonality in temperate and subtropical China.

Methods: We used weekly surveillance data on influenza virus activity in mainland China and Hong Kong from 2005 through 2016. We estimated the transmissibility via the instantaneous reproduction number (R_t), a real-time measure of transmissibility, and examined its relationship with different climactic drivers and allowed for the timing of school holidays and the decline in susceptibility in the population as an epidemic progressed. We developed a multivariable regression model for R_t to quantify the contribution of various potential environmental drivers of transmission.

Findings: We found that absolute humidity is a potential driver of influenza seasonality and had a U-shaped association with transmissibility and hence can predict the pattern of influenza virus transmission across different climate zones. Absolute humidity was able to explain up to 15% of the variance in R_t, and was a stronger predictor of R_t across the latitudes. Other climatic drivers including mean daily temperature explained up to 13% of variance in R_t and limited to the locations where the indoor measures of these factors have better indicators of outdoor measures. The non-climatic driver, holiday-related school closures could explain up to 7% of variance in R_t.

Interpretation: A U-shaped association of absolute humidity with influenza transmissibility was able to predict seasonal patterns of influenza virus epidemics in temperate and subtropical locations.

* Corresponding author at: School of Public Health, Li Ka Shing Faculty of Medicine, The University of Hong Kong, 7 Sassoon Road, Pokfulam, Hong Kong Special Administrative Region.
E-mail address: bcowling@hku.hk (B.J. Cowling).

https://doi.org/10.1016/j.scitotenv.2021.151724

Please cite this article as: S.T. Ali, B.J. Cowling, J.Y. Wong, et al., Influenza seasonality and its environmental driving factors in mainland China and Hong Kong, Science of the Total Environment, https://doi.org/10.1016/j.scitotenv.2021.151724

1. Introduction

In temperate regions influenza virus epidemics occur annually in winter months (Tamerius et al., 2011), while seasonality is more variable in tropical and subtropical locations often with multiple epidemic peaks were seen each year (Azziz Baumgartner et al., 2012; Tamerius et al., 2011; Tan et al., 2014; Yang et al., 2008). For example, the influenza epidemics in Hong Kong tend to occur in winter months of December–March and summer months of May–September (Chong et al., 2015; Cowling et al., 2006; Lau et al., 2008; Wu et al., 2012). An important factor affecting seasonal influenza transmission is population immunity (Earn et al., 2002; Xia et al., 2005), which gradually increases as epidemic progresses and is one of the main reasons an epidemic eventually comes to an end (Dowell, 2001; Lipsitch and Viboud, 2009; Lofgren et al., 2007; Tamerius et al., 2011). Climatic factors are also thought to play a role in the seasonality of influenza epidemics. Temperature and humidity have both been shown to have direct effects on virus survival (Lowen and Steel, 2014; Lowen et al., 2007; Shaman and Kohn, 2009; Tamerius et al., 2013; te Beest et al., 2013a). In addition, there is greater indoor crowding in the winter (Lofgren et al., 2007), and potential changes in host immunity at different times of the year, able to drive the influenza seasonality (Dowell, 2001; Lipsitch and Viboud, 2009; Lofgren et al., 2007; Tamerius et al., 2011).

Studying patterns in influenza activity in different locations provides an opportunity to examine potential climatic drivers of influenza transmission and seasonality. The time-varying transmissibility of influenza can be characterized by the instantaneous (or effective) reproduction number, R_t, defined as the average number of secondary infections caused by a typical single infectious individual at time t. In this study, we analyzed surveillance data on influenza virus activity in 8 locations in mainland China plus Hong Kong during the period from Oct 2005 through Apr 2016, using regression models to quantify the influence of various factors on time-varying transmissibility measured by R_t. The objective of our study was to identify the potential climatic drivers of influenza transmission in these locations, and to quantify their influence on the influenza seasonality in temperate and subtropical locations.

2. Materials and methods

2.1. Influenza surveillance data

We collected the weekly proportion of outpatient consultations due to influenza like illness (ILI) and the weekly proportion of sentinel specimens tested positive for influenza viruses in Hong Kong and mainland China from 3 October 2005 through 3 April 2016. The ILI data in selected provinces and municipalities in mainland China were retrieved from a previously published study (Feng et al., 2020) while the data in Hong Kong were obtained from the Centre for Health Protection of the Hong Kong Special Administrative Region based on the influenza sentinel surveillance network.

We obtained a proxy measures of influenza virus activity in the community, referred to as ILI+ rates, by multiplying together the ILI rates with the proportions of influenza-positive specimens (Goldstein et al., 2011). This time series should be a reasonable linear correlate of the incidence rate of infections in the community, and it was previously shown that there was a very close correlation between this measure and laboratory confirmed H1N1pdm09 hospitalizations in Hong Kong in 2009–10 (Wong et al., 2013). Finally, we multiplied the weekly ILI+ rates by a constant, representing the inverse of the estimated coverage of the sentinel sites in these locations, and rounded to the nearest integer to obtain a time series of weekly ILI+ counts. We used the constant to scale up the ILI+ counts to values consistent with the expected incidence rates of infections in the population (Ali et al., 2018a; Ali et al., 2018b; Ryu et al., 2020; Wong et al., 2013; Wu et al., 2017).

We restricted our analysis to 8 Chinese provinces and municipalities plus Hong Kong (Fig. 1). We have selected these locations based on the geographical diversity and availability of influenza surveillance data across the study period. Given their geoclimatic characteristics, Beijing, Tianjin and Gansu were classified as temperate locations at higher latitudes, Shanghai, Zhejiang, and Hubei as temperate locations at medium latitudes, and Jiangxi, Guangdong and Hong Kong as subtropical locations at lower latitudes.

We defined influenza epidemics as periods of at least seven or more consecutive weeks during which an epidemic threshold was exceeded. The epidemic threshold was determined as the 50th percentile of all the non-zero weekly ILI+ counts over the study period (Fig. 2) (Ali et al., 2018a; Yang et al., 2015). We interpolated the cumulative weekly ILI+ counts data to obtain the daily ILI+ cumulative counts using spline functions and finally evaluated the daily ILI+ count data, as the measure of transmissibility is defined by the daily number of cases accounting for the mean infectious period (less than a week for influenza) of the infectors (Ali et al., 2018a; Ali et al., 2018b; Ryu et al., 2020; te Beest et al., 2013b).

2.2. Meteorological data

Daily meteorological drivers including mean air pressure, mean relative humidity, mean air temperature were retrieved for the period 2005 through 2016 from the China Meteorological Administration and the Hong Kong Observatory. We derived the daily mean absolute humidity from the mean relative humidity and mean temperature (Wu et al., 2012), and then obtained the weekly absolute humidity as the arithmetic mean of the daily absolute humidity in that week. We also retrieved mean hour-sunshine, mean wind speed and direction of maximum wind speed for the locations in mainland China and mean cloud cover, mean dew point, and mean rainfall for Hong Kong.

2.3. School holiday data

We retrieved the information on holiday-related school closures in each location studied, including the Chinese New Year holidays, the winter holidays, the summer holidays and the public holidays (national and provincial level) throughout our study period. Along with these regular school holidays we also included the dates of additional school closures during the 2008 influenza epidemic (Cowling et al., 2008) and the 2009 influenza pandemic (Wu et al., 2010), in Hong Kong in our analysis.

2.4. Estimation of the daily instantaneous reproduction number, R_t

Transmissibility can be measured by the instantaneous reproduction number (R_t), defined as the average number of secondary infections caused by a typical single infectious person at time t. We estimated R_t from daily ILI+ counts using a simple branching process model (Cori et al., 2013). We assumed the serial interval for influenza followed a Gamma distribution with a mean of 2.6 days and a standard deviation of 1.5 days (Cauchemez et al., 2009).

2.5. Exploratory data analysis with R_t

We assessed the best-fitting functional forms for the association between R_t and each meteorological driver for each location by fitting linear, exponential and power forms of univariate regression models with lags of 0 to 14 days to account for reporting delays (Ali et al., 2018a; te Beest et al., 2013b). The significant drivers with their best-fitted functional form were selected based on the Akaike Information Criterion (AIC) rule for K-L (Kullback-Leibler) best model by evaluating AIC difference $\Delta_i = \Delta\ AIC_i = AIC_i - AIC_{min}$, where, $i=$ linear, exponential and power forms of association and $AIC_{min} = min\ (AIC_{Linear}, AIC_{Exponential}, AIC_{Power})$ (Ali et al., 2018a). Further, we used

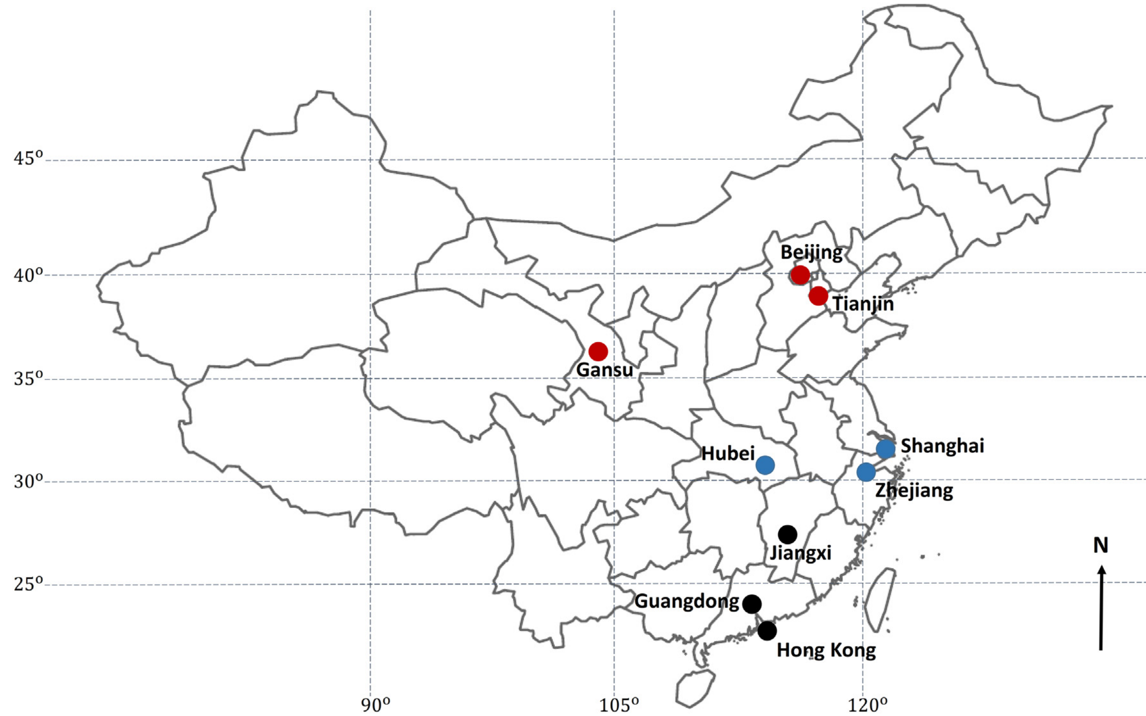

Fig. 1. The map indicating the locations studied in mainland China and Hong Kong. The colour indicates the latitude: high-latitude (in red), mid-latitude (in blue), and low-latitude (in black). The latitude of each location was recorded as the latitude of the corresponding provincial capitals. (For interpretation of the references to colour in this figure legend, the reader is referred to the web version of this article.)

combined data of all locations together to establish the general model of association between R_t and meteorological drivers and predicted the influenza circulation patterns as either single or double peaks in the study years in these locations. To assess whether these associations were due to chance, we performed permutation analysis on these regression models with 1000 dummy or null scenarios and compared the results with one true time series.

2.6. Multivariable regression analysis with R_t

We used a multivariable log-linear regression model incorporating depletion of susceptibles over time and inter-epidemic effects in basic model first as described in the Appendix. We then fitted improved models including the significant meteorological drivers. We quantified the impact of individual drivers by comparing R-square (R^2) values for the basic and improved models. We evaluated R^2 values by using the best lag (i.e. the lag for which the model has the largest R^2 value) and a distributed lag model (DLM, through the dlnm package in R), where the latter summarizes the overall effect distributed over multiple days instead of just reporting the results with the single best lag. This distributed modeling framework similarly accounts the likelihood of infections in previous days (at least a mean generation time) to measure of transmissibility R_t. We considered data from maximum of 6 weeks (5 to 7 weeks for sensitivity analyses) either sides of the peak in the multivariable regression models to avoid the effects of the low and irregular reporting during the very beginning and end of each epidemic.

2.7. Analysis with adjusted R_t

In theory, R_t is driven by depletion of susceptibles and tends to gradually decrease as an epidemic progress. We evaluated the adjusted R_t by eliminating the effect of depletion of susceptibles from R_t. As explained in the Appendix, we first fitted a simple model including only depletion of susceptibles to the estimated R_t for each epidemic separately, and evaluated the adjusted R_t as the residual of the fit. This measure of adjusted R_t is controlled for the effects of depletion of susceptibles and driven by the inter-epidemic effects and the possible extrinsic drivers. We then performed the above regression analyses on adjusted R_t.

3. Results

The time series of ILI+ counts for Hong Kong and different locations in mainland China are shown in Fig. 2 for the period from 3 October 2005 through 3 April 2016. We identified 10 distinct influenza epidemics for Beijing, 11 for Tianjin, 10 for Gansu, 13 for Shanghai, 14 for Zhejiang, 13 for Hubei, 13 for Jiangxi, 10 for Guangdong, 11 for Hong Kong with different lengths and patterns (single or double peaks), which covered an average of 78% of the total study period.

We quantified the transmissibility (R_t) for influenza during these epidemics for each location. The median values of R_t across all epidemics for these locations ranged between 1.02 (95% CrI: 0.51, 1.56) and 1.07 (95% CrI: 0.60, 1.67), with maximum values ranged between 2.18 (95% CrI: 1.02, 4.39) and 2.52 (95% CrI: 1.13, 4.79) at the start of an epidemic and the minimum values ranged between 0.35 (95% CrI: 0.22, 0.59) and 0.43 (95% CrI: 0.29, 0.67) at the end of epidemics.

We explored the association between influenza transmissibility, as measured by R_t and each factor with lagged values of 0–14 days for each location. The estimated AIC differences ($\triangle_i$) indicated that the exponential and power form of non-linear association better represented the effect of the meteorological drivers on influenza transmissibility (Table S5). In some locations including Hong Kong, Hubei, and Zhejiang the absolute humidity indicated exponential forms were better over power forms. The mean air pressure, mean relative humidity, mean temperature and mean absolute humidity are found to be significant drivers across the locations. These significant drivers were included in further analysis.

The analysis of general model using combined data suggested absolute humidity as a significant driver of influenza transmission. The U-shaped form of this general model for the locations studied indicates the influenza transmissibility is higher during periods with low or

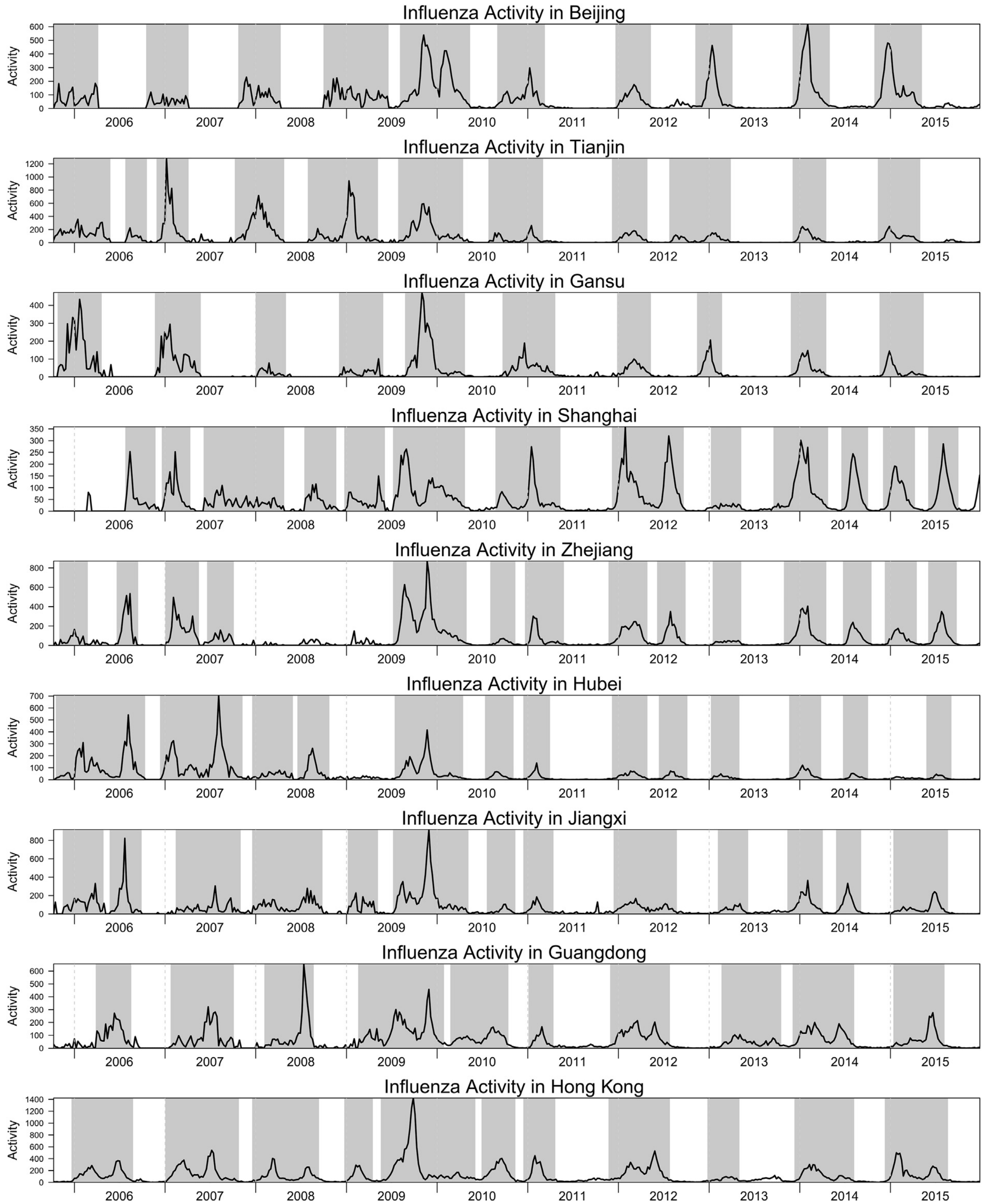

Fig. 2. Weekly influenza activity as ILI + counts (black lines) along with the predefined epidemics (grey shaded area) in 8 different locations in mainland China plus Hong Kong from Oct 2005 through Apr 2016.

high ambient absolute humidity, but lower with moderate humidity (Fig. 3a and b). The permutation analysis on the 1000 null/dummy time series of absolute humidity was able to explain substantially less variance in transmissibility compared to the observed true time series (Fig. 3c). We noticed the variation by latitude in prediction of the transmissibility and the pattern of influenza virus circulation (reflecting single and multiple peaks) over the periods based on ambient absolute humidity (Fig. 4).

In multivariable regression analysis of R_t stratified by location, the models could explain 24% - 52% of the observed variation in estimated reproduction numbers (R_t). A considerable fraction of the observed variance (14%–43%) in R_t was explained by the basic model including depletion of susceptibles and inter-epidemic effects (Table 1). Inclusion of the meteorological drivers in the multivariable regression model improved the model fit (R^2) marginally, explaining up to 5% -17% of the variance in R_t across the locations studied (Table 1). Similar results

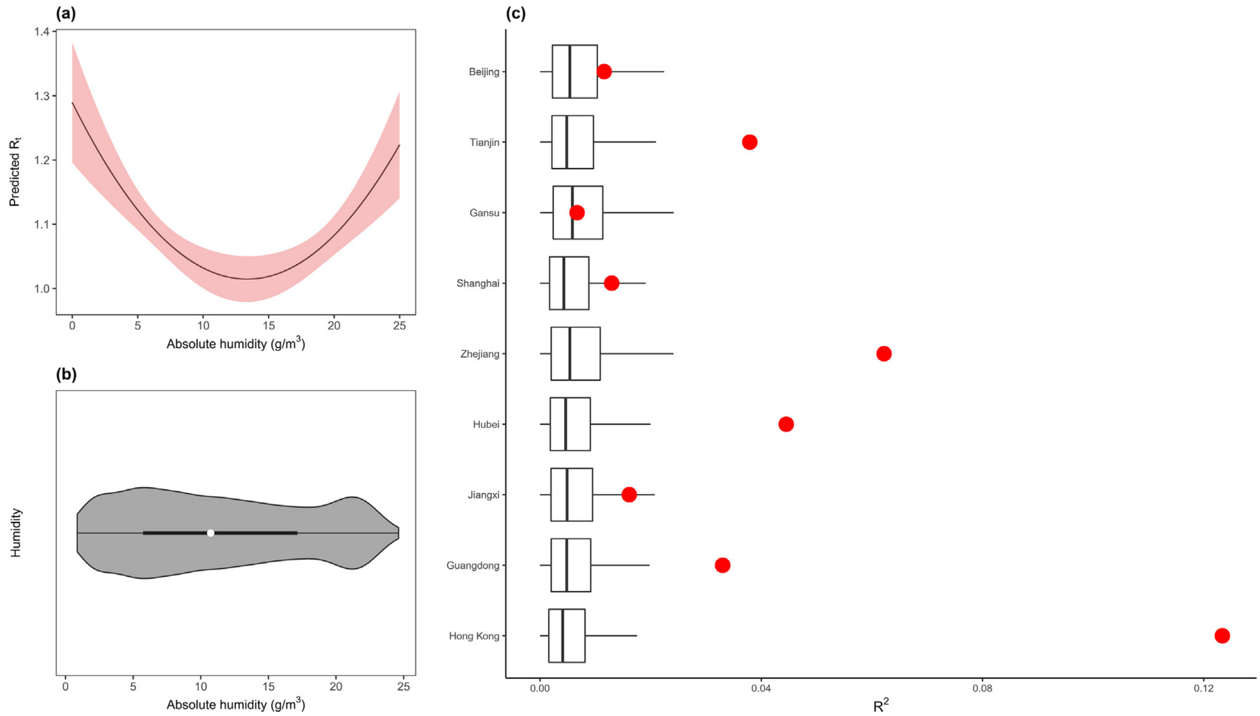

Fig. 3. (a) The predicted general U-shaped form (black line) with 95% CI (shaded region) of association for absolute humidity on influenza transmissibility; (b) violin plot of combined absolute humidity across all the 9 locations. (c) Percentage of the variance of the instantaneous reproduction number (R_t) explained by 1000 null/dummy time series (respective boxplot) and a true time series (bold red dots) of absolute humidity in permutation test. The true time series of ambient absolute humidity is explaining significantly larger variance in R_t compare to that of by null/dummy time series of absolute humidity. (For interpretation of the references to colour in this figure legend, the reader is referred to the web version of this article.)

were noted for the analysis on R_t adjusted for depletion of susceptible (Table 1, S6 and S7). Compared with the best lag models, the distributed lag models explained higher variation in transmissibility by these drivers (Table 1, S6 and S7). In a sensitivity analysis, inclusion of data from 5 to 7 weeks at either side of the epidemic peak led to similar findings (Table 1, S6).

4. Discussion

We assessed the influenza transmissibility in 8 geographically diverse locations in mainland China along with Hong Kong (Fig. 1). The inter-location (by latitude) differences in average ambient temperature, humidity (relative and absolute) and population sizes were clearly noticeable across the last 3 decades (Tables S1–S4). Within each location the annual averages of these meteorological drivers were much comparable (Tables S1–S3) but the variations in daily/weekly measures were evident (Fig. 1). We used the time series of influenza surveillance data during October 2005 through April 2016, to understand the transmission dynamics and driving factors of influenza seasonality accounting for geographical diversity in climate. Influenza often caused regular winter epidemics in temperate regions such as Europe and North America (Lau et al., 2008; Tamerius et al., 2013; Tang et al., 2010), but showed less regular seasonality in tropical and subtropical regions (Tamerius et al., 2011; Tamerius et al., 2013). Influenza circulated throughout the year in subtropical locations and was not limited to winter periods (Fig. 2). Change in depletion of susceptibles is one of the key drivers affecting the transmissibility of influenza virus during an epidemic, while other extrinsic drivers might have further contribution to changes in transmissibility. Small changes in transmissibility associated with these seasonal climatic drivers could lead to large oscillations in incidence of influenza (Dushoff et al., 2004).

We analyzed in total 105 epidemics during the study period, The range of transmissibility (R_t) for these epidemics was found to be fairly consistent across the locations and very similar to the earlier estimates in mainland China, Hong Kong (Cowling et al., 2010; Wu et al., 2010) and elsewhere (Boelle et al., 2011). Our univariate regression analysis revealed that ambient absolute humidity had a non-linear relationship on the transmissibility across the locations studied. We noticed the lower AIC values for non-linear models of these driving factors (SI Appendix, Table S5). There was a negative association (the left-hand side of the U-shaped form of association) between transmissibility and absolute humidity in high-latitude locations (e.g. Beijing, Tianjin and Gansu), whereas in low-latitude (e.g. Hong Kong, Guangdong and Jiangxi) and mid-latitude (e.g. Shanghai, Hubei and Zhenjiang) locations we found a U-shaped association as the best fitting models of the absolute humidity on transmissibility. This form of association of absolute humidity with transmissibility could predict the influenza transmission in these location by capturing the single winter season in high-latitude locations and multiple seasons in low-latitude and mid-latitude locations (Fig. 4).

Ambient temperature and humidity were reported to have potential role in modulating the viability and stability of respiratory viruses including influenza by affecting the properties of viral surface proteins and lipid membrane and proportion of droplet nuclei (Marr et al., 2019; Shaman and Kohn, 2009). In animal transmission studies, at equilibrium state, the high (>60%) as well as low (<40%) relative humidity were found to improve the viability of influenza viruses in droplets compared with intermediate relative humidity (40% to 60%) under which viruses were more quickly inactivated (Lowen and Palese, 2009; Lowen et al., 2007; Lowen et al., 2008; Moriyama et al., 2020). Whereas, viral stability found to be a good correlate with low relative humidity (20% to 50%) during winter and higher relative humidity (80%) during summer (Harper, 1961; Moriyama et al., 2020). In an analytical chemical study, the low-temperature was found to promote the ordering of lipids on the viral membrane and contributed to the stability of the influenza virus particles (Polozov et al., 2008). In a recent animal study, several mechanisms were explored to quantify the impact of low humidity in host immunity and susceptibility. Mucociliary

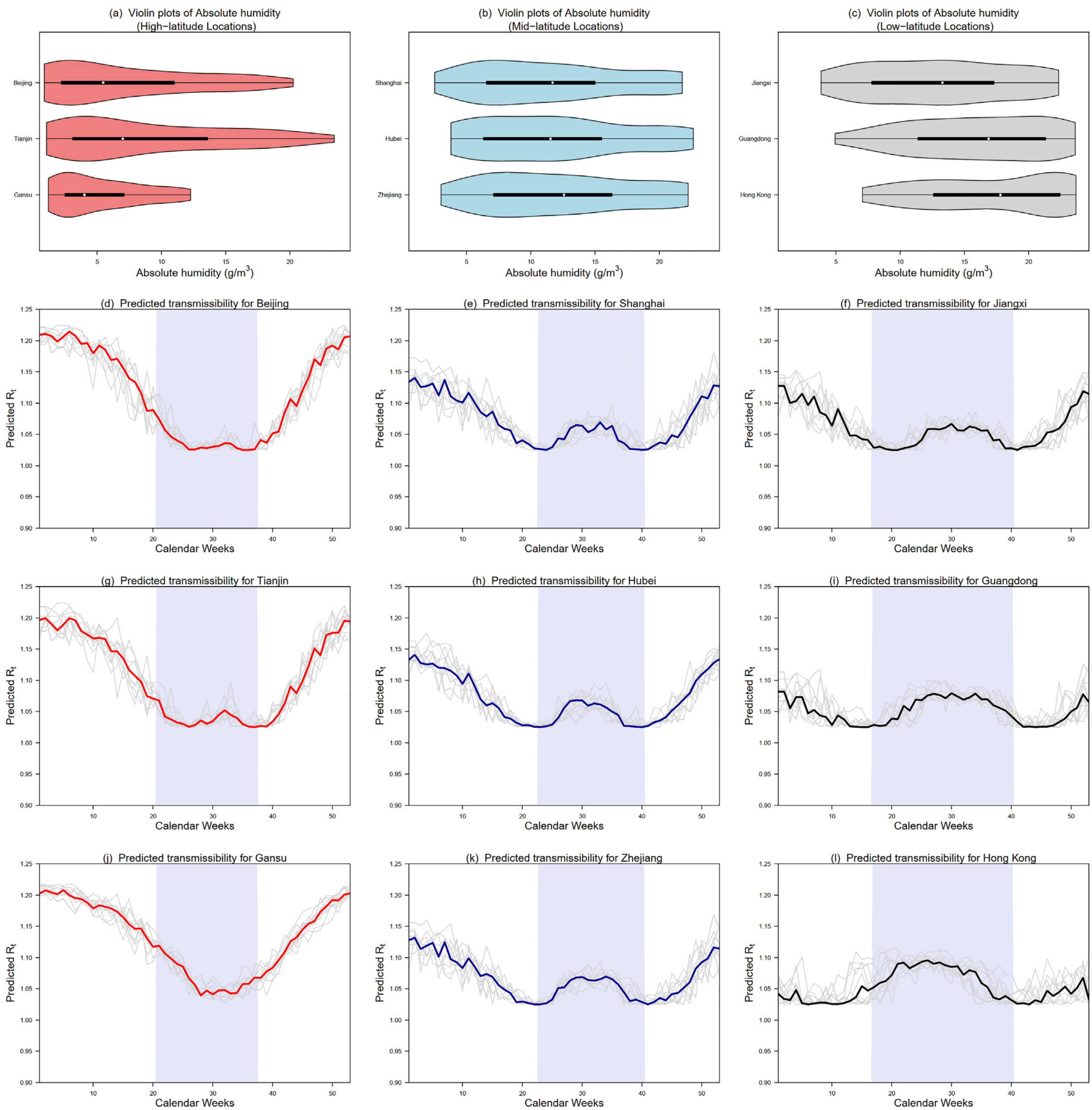

Fig. 4. Absolute humidity driven prediction of transmissibility of influenza in different locations. (a-c) The violin plots of absolute humidity for respective 9 locations: (a) for three high-latitude locations (Beijing, Tianjin and Gansu), (b) for three mid-latitude locations (Shanghai, Hubei and, Zhenjiang), and (c) for low-latitude locations (Jiangxi, Guangdong, and Hong Kong). (d–l) The absolute humidity driven prediction of yearly transmissibility (each year predictions in grey lines and average yearly predictions in bold lines) for the respective locations; summer seasons are indicated by shaded regions of light violet colour. For high-latitude locations the model could predict the sole winter epidemics, while in mid and low latitude locations model could mimic both winter and summer epidemics with comparatively prominent transmission during summer in low-latitude locations. (For interpretation of the references to colour in this figure legend, the reader is referred to the web version of this article.)

clearance and airway tissue repair mechanisms could severely impaired at low humidity, and dry air exposure could reduce global ISG expressions following intranasal influenza virus infection (Kudo et al., 2019). On the other hand, the studies suggested that the indoor temperature could affect the adaptive immune responses in host in general (Eng et al., 2015; Kokolus et al., 2013). A high ambient temperature could weaken the virus-specific adaptive immunity following influenza virus infection possibly reflecting the summer epidemics occurred in some places (Moriyama and Ichinohe, 2019).

A study in 1960 reported indoor relative humidity as an important environmental factor for virus survival in aerosols and could explain the seasonality of influenza virus (Hemmes et al., 1960). A more recent study explored how relative humidity was more likely than absolute humidity to modulate influenza virus survival and transmissibility (Marr et al., 2019). Based on the physical and chemical characteristics of droplets and survival mechanism of the virus, outdoor absolute humidity was found to be a comparable proxy for indoor relative humidity in temperate regions during wintertime heating seasons (Marr et al., 2019). In

Table 1
Percentage of the variance of the instantaneous reproduction number (R_t) explained by the meteorological drivers, from models on pre-defined influenza epidemics with a maximum duration of 6 weeks (in brackets the range of the estimates based on 5–7 weeks) to both side of peaks for epidemics in respective locations from Oct 2005 through Apr 2016. The results based on the distributed lag model (DLM) with lags of 0–2 weeks.

Locations	Models	With unadjusted R_t			With adjusted R_t		
		R^2	$\%\Delta R^2$	*df*	R^2	$\%\Delta R^2$	*df*
Beijing	Basic Model[a]	0.19 (0.14, 0.19)	–	119 (102, 138)	0.06 (0.05, 0.07)	–	129 (112, 148)
	Abs. humidity[b]	0.23 (0.16, 0.23)	4 (2, 5)	113 (96, 132)	0.16 (0.13, 0.31)	10 (8, 24)	123 (106, 142)
	School holidays[b]	0.21 (0.16, 0.17)	2 (1, 2)	113 (96, 132)	0.07 (0.05, 0.07)	1 (0, 1)	123 (106, 142)
	All drivers[c]	0.24 (0.22, 0.28)	5 (4, 13)	107 (90, 108)	0.16 (0.15, 0.35)	10 (9, 30)	117 (100, 118)
Tianjin	Basic Model[a]	0.43 (0.33, 0.46)	–	114 (99, 130)	0.05 (0.05, 0.06)	–	125 (110, 141)
	Abs. humidity[b]	0.50 (0.39, 0.53)	7 (6, 7)	108 (93, 124)	0.09 (0.08, 0.13)	4 (3, 8)	119 (104, 135)
	School holidays[b]	0.45 (0.35, 0.49)	2 (2,3)	108 (93, 124)	0.11 (0.07, 0.14)	6 (1, 9)	119 (104, 135)
	All drivers[c]	0.52 (0.42, 0.56)	9 (9, 10)	102 (87, 118)	0.15 (0.11, 0.21)	10 (6, 15)	113 (98, 129)
Gansu	Basic Model[a]	0.29 (0.25, 0.31)	–	107 (89, 122)	0.06 (0.05, 0.07)	–	117 (99, 132)
	Abs. humidity[b]	0.35 (0.32, 0.37)	6 (6,7)	101 (83, 116)	0.11 (0.09, 0.11)	5 (4, 5)	111 (93, 126)
	School holidays[b]	0.36 (0.35, 0.38)	7 (7, 10)	101 (83, 116)	0.16 (0.15, 0.22)	11 (11, 15)	111 (93, 126)
	All drivers[c]	0.41 (0.41, 0.45)	12 (12, 15)	95 (77, 110)	0.21 (0.20, 0.26)	16 (15, 19)	105 (87, 120)
Shanghai	Basic Model[a]	0.34 (0.33, 0.34)	–	183 (165, 202)	0.02 (0.02, 0.02)	–	196 (178, 215)
	Abs. humidity[b]	0.41 (0.41, 0.42)	7 (7, 9)	177 (159, 196)	0.05 (0.05, 0.07)	3 (3, 4)	190 (172, 209)
	School holidays[b]	0.35 (0.35, 0.36)	1 (1, 3)	177 (159, 196)	0.05 (0.05, 0.08)	3 (3, 5)	190 (172, 209)
	All drivers[c]	0.42 (0.42, 0.54)	8 (8, 20)	171 (135, 190)	0.11 (0.10, 0.22)	9 (8, 19)	184 (148, 203)
Zhejiang	Basic Model[a]	0.38 (0.38, 0.41)	–	153 (138, 177)	0.08 (0.07, 0.08)	–	167 (152, 191)
	Abs. humidity[b]	0.44 (0.44, 0.51)	6 (6, 9)	147 (132, 171)	0.15 (0.13, 0.15)	7 (5, 7)	161 (146, 185)
	School holidays[b]	0.41 (0.41, 0.45)	3 (2, 4)	147 (132, 171)	0.10 (0.09, 0.10)	1 (0, 1)	161 (146, 185)
	All drivers[c]	0.47 (0.44, 0.55)	10 (8, 14)	141 (126, 165)	0.17 (0.14, 0.17)	8 (7, 8)	155 (140, 179)
Hubei	Basic Model[a]	0.31 (0.26, 0.31)	–	194 (174, 213)	0.02 (0.02, 0.08)	–	207 (152, 226)
	Abs. humidity[b]	0.36 (0.28, 0.36)	5 (2, 5)	188 (168, 207)	0.04 (0.04, 0.15)	2 (2, 7)	201 (146, 220)
	School holidays[b]	0.34 (0.29, 0.34)	3 (3, 4)	188 (168, 207)	0.05 (0.05, 0.09)	3 (1, 3)	201 (146, 220)
	All drivers[c]	0.40 (0.32, 0.40)	9 (6, 10)	182 (162, 201)	0.13 (0.12, 0.14)	10 (10, 11)	195 (175, 214)
Guangdong	Basic Model[a]	0.23 (0.16, 0.23)	–	199 (180, 216)	0.05 (0.02, 0.05)	–	209 (190, 226)
	Abs. humidity[b]	0.27 (0.20, 0.27)	4 (3, 4)	193 (174, 214)	0.06 (0.04, 0.06)	1 (1, 2)	203 (184, 220)
	School holidays[b]	0.24 (0.17, 0.24)	1 (0, 1)	193 (174, 214)	0.08 (0.03, 0.08)	3 (0, 3)	203 (184, 220)
	All drivers[c]	0.28 (0.21, 0.28)	5 (4, 5)	187 (168, 212)	0.10 (0.05, 0.10)	5 (2, 5)	197 (178, 214)
Jiangxi	Basic Model[a]	0.14 (0.14, 0.15)	–	218 (201, 236)	0.06 (0.06, 0.07)	–	231 (214, 249)
	Abs. humidity[b]	0.18 (0.18, 0.19)	4 (3, 4)	211 (194, 229)	0.09 (0.08, 0.09)	3 (2, 3)	224 (207, 242)
	School holidays[b]	0.19 (0.18, 0.20)	5 (4, 5)	212 (194, 229)	0.16 (0.16, 0.18)	10 (10, 11)	225 (208, 243)
	All drivers[c]	0.24 (0.21, 0.25)	10 (7, 10)	205 (187, 222)	0.20 (0.19, 0.22)	14 (14, 15)	218 (201, 236)
Hong Kong	Basic Model[a]	0.35 (0.33, 0.36)	–	209 (188, 299)	0.02 (0.2, 0.2)	–	220 (199, 240)
	Abs. humidity[b]	0.50 (0.48, 0.51)	15 (12, 18)	203 (182, 223)	0.08 (0.08, 0.09)	6 (6, 7)	214 (193, 234)
	School holidays[b]	0.37 (0.35, 0.38)	2 (2, 3)	203 (182, 223)	0.07 (0.07, 0.08)	5 (5, 6)	214 (193, 234)
	All drivers[c]	0.52 (0.49, 0.53)	17 (14, 20)	197 (176, 217)	0.12 (0.12, 0.14)	10 (10, 12)	208 (187, 228)

R^2 and *df* are measures of R-square and degree of freedom from the multivariable regression model respectively. $\%\Delta R^2$ measured the change in the explained variance (of total variance) from the model in comparison to the basic model. i.e. $\%\Delta R^2 = (R^2_{improved\ models} - R^2_{basic\ model}) \times 100$.

[a] Basic Model: factors affecting R_t (or adjusted R_t) include depletion of susceptibles, and/or inter-epidemic factors.

[b] Improved models include the basic model for R_t plus the respective drivers.

[c] Improved model includes the drivers: mean absolute humidity and school holiday (statistically significant and free from multicollinearity).

recent decades, studies suggested that the outdoor absolute humidity as a potential driver of influenza transmission could modulate influenza virus survival and hence influenza transmission and seasonality across the latitudes (Deyle et al., 2016; McDevitt et al., 2010; Shaman and Kohn, 2009; Shaman et al., 2010). Our general model for absolute humidity on transmissibility supports previous laboratory experiments on temperate and global influenza transmission (Dalziel et al., 2018; Shaman and Kohn, 2009; Shaman et al., 2011; Tamerius et al., 2013) where the virus survivability increased during low (0–12 g/m^3 in temperate and tropical climates) and high levels (18–24 g/m^3 in tropical climates) of ambient absolute humidity (Shaman and Kohn, 2009; te Beest et al., 2013a; Prussin et al., 2018; Shaman et al., 2011). While most transmissions likely occur indoors, but indoor and outdoor temperatures correlate well only at warmer outdoor temperatures. The outdoor relative humidity is a poor indicator of indoor relative humidity, whereas indoor absolute humidity has a strong correlation with outdoor absolute humidity year-round (Nguyen et al., 2014). Further, outdoor ambient absolute humidity is likely to be a good correlate with indoor relative humidity that affects virus survival (Marr et al., 2019). Moreover, the indoor measures of these drivers are not consistent even in same location and often not readily available, therefore, we restricted our main analysis with outdoor absolute humidity.

In the multivariable regression analysis with R_t, we found that a substantial amount of observed variance in estimated transmissibility (R_t) was explained by the inclusion of external factors including school holidays and climatic factors (Table 1). School holidays were also associated with reductions in transmissibility, consistent with a wealth of literature on the importance of children in influenza transmission and the impact of school holidays and closures (Ali et al., 2018b; Cowling et al., 2008; Wu et al., 2010; Cauchemez et al., 2008). Mechanistically, mean temperature could even potentially explain a substantial part of the variance in R_t when indoor and outdoor temperatures are well correlated, which is possibly true for summer in high-latitude and winter in lower-latitude locations. While absolute humidity could explain a considerable variance in R_t for any locations in general, the outdoor measures of absolute humidity were suggested to be a good correlate of its indoor measures (Nguyen et al., 2014). These results suggested that low absolute humidity (often determined by low temperature and low relative humidity) might drive the winter influenza circulation in temperate as well as sub-tropical locations, and that high absolute humidity might play an important role in summer epidemics in subtropical and tropical locations.

A potential limitation of our study is that we inferred transmissibility from aggregated surveillance data, and we were not able to assess the possible effects of different age groups or more detailed social or demographic factors in transmission dynamics. Furthermore, we did not have information on the specific influenza strains that circulated in these locations in different epidemics, which would have allowed more precise analyses particularly of population immunity since that would be largely strain-specific. Finally, although the nine locations included in our analysis, our findings represented a wide range of latitude and we would not expect different observations in other parts of mainland China, observations from other parts of the world would also be valuable.

5. Conclusions

In conclusion, by using influenza transmissibility instead of reported cases or incidence, we identified absolute humidity one of the potential drivers of influenza seasonality in geographically diverse locations in mainland China and Hong Kong. Other significant drivers included mean air temperature, relative humidity, air pressure and school holidays. The U-shaped association between absolute humidity and influenza transmissibility could contribute to a general model to predict the annual (in temperate regions) and bi-annual (in subtropics and tropics) circulation of influenza virus.

CRediT authorship contribution statement

Conception: STA, BJC and PW. Data collection: STA. Data analysis: STA and DC. Wrote first draft: STA. Critically revised manuscript and approved final version: All authors.

Declaration of competing interest

BJC received honoraria from Sanofi, Roche, AstraZeneca, Moderna and GSK. The authors report no other potential conflicts of interest.

Acknowledgments

The authors thank Julie Au and Vicky Fang for technical assistance. This project was supported by the General Research Fund of the Hong Kong Research Grants Council (project no. 17106617), the Health and Medical Research Fund (project no. 18171202), and a commissioned grant from the Health and Medical Research Fund from the Government of the Hong Kong Special Administrative Region. The funding bodies had no role in study design, data collection and analysis, preparation of the manuscript, or the decision to publish.

Appendix A. Supplementary data

Supplementary data to this article can be found online at https://doi.org/10.1016/j.scitotenv.2021.151724.

References

Ali, S.T., Wu, P., Cauchemez, S., et al., 2018. Ambient ozone and influenza transmissibility in Hong Kong. Eur. Respir. J. 51 (5).

Ali, S.T., Cowling, B.J., Lau, E.H.Y., Fang, V.J., Leung, G.M., 2018. Mitigation of influenza B epidemic with school closures, Hong Kong, 2018. Emerg. Infect. Dis. 24 (11), 2071–2073.

Azziz Baumgartner, E., Dao, C.N., Nasreen, S., et al., 2012. Seasonality, timing, and climate drivers of influenza activity worldwide. J. Infect. Dis. 206 (6), 838–846.

Boelle, P.Y., Ansart, S., Cori, A., Valleron, A.J., 2011. Transmission parameters of the A/H1N1 (2009) influenza virus pandemic: a review. Influenza Other Respir. Viruses 5 (5), 306–316.

Cauchemez, S., Valleron, A.J., Boelle, P.Y., Flahault, A., Ferguson, N.M., 2008. Estimating the impact of school closure on influenza transmission from sentinel data. Nature 452 (7188), 750–754.

Cauchemez, S., Donnelly, C.A., Reed, C., et al., 2009. Household transmission of 2009 pandemic influenza a (H1N1) virus in the United States. N. Engl. J. Med. 361 (27), 2619–2627.

Chong, K.C., Goggins, W., Zee, B.C., Wang, M.H., 2015. Identifying meteorological drivers for the seasonal variations of influenza infections in a subtropical city - Hong Kong. Int. J. Environ. Res. Public Health 12 (2), 1560–1576.

Cori, A., Ferguson, N.M., Fraser, C., Cauchemez, S., 2013. A new framework and software to estimate time-varying reproduction numbers during epidemics. Am. J. Epidemiol. 178 (9), 1505–1512.

Cowling, B.J., Wong, I.O., Ho, L.M., Riley, S., Leung, G.M., 2006. Methods for monitoring influenza surveillance data. Int. J. Epidemiol. 35 (5), 1314–1321.

Cowling, B.J., Lau, E.H., Lam, C.L., et al., 2008. Effects of school closures, 2008 winter influenza season, Hong Kong. Emerg. Infect. Dis. 14 (10), 1660–1662.

Cowling, B.J., Lau, M.S., Ho, L.M., et al., 2010. The effective reproduction number of pandemic influenza: prospective estimation. Epidemiology 21 (6), 842–846.

Dalziel, B.D., Kissler, S., Gog, J.R., et al., 2018. Urbanization and humidity shape the intensity of influenza epidemics in U.S. Cities. Science 362 (6410), 75–79.

Deyle, E.R., Maher, M.C., Hernandez, R.D., Basu, S., Sugihara, G., 2016. Global environmental drivers of influenza. Proc. Natl. Acad. Sci. U. S. A. 113 (46), 13081–13086.

Dowell, S.F., 2001. Seasonal variation in host susceptibility and cycles of certain infectious diseases. Emerg. Infect. Dis. 7 (3), 369–374.

Dushoff, J., Plotkin, J.B., Levin, S.A., Earn, D.J., 2004. Dynamical resonance can account for seasonality of influenza epidemics. Proc. Natl. Acad. Sci. U. S. A. 101 (48), 16915–16916.

Earn, D.J.D., Dushoff, J., Levin, S.A., 2002. Ecology and evolution of the flu. Trends Ecol. Evol. 17 (7), 334–340.

Eng, J.W., Reed, C.B., Kokolus, K.M., et al., 2015. Housing temperature-induced stress drives therapeutic resistance in murine tumour models through beta2-adrenergic receptor activation. Nat. Commun. 6, 6426.

Feng, L., Feng, S., Chen, T., et al., 2020. Burden of influenza-associated outpatient influenza-like illness consultations in China, 2006–2015: a population-based study. Influenza Other Respir. Viruses 14 (2), 162–172.

Goldstein, E., Cobey, S., Takahashi, S., Miller, J.C., Lipsitch, M., 2011. Predicting the epidemic sizes of influenza A/H1N1, A/H3N2, and B: a statistical method. PLoS Med. 8 (7), e1001051.

Harper, G.J., 1961. Airborne micro-organisms: survival tests with four viruses. J. Hyg. (Lond.) 59, 479–486.

Hemmes, J.H., Winkler, K.C., Kool, S.M., 1960. Virus survival as a seasonal factor in influenza and polimyelitis. Nature 188, 430–431.

Kokolus, K.M., Capitano, M.L., Lee, C.T., et al., 2013. Baseline tumor growth and immune control in laboratory mice are significantly influenced by subthermoneutral housing temperature. Proc. Natl. Acad. Sci. U. S. A. 110 (50), 20176–20181.

Kudo, E., Song, E., Yockey, L.J., et al., 2019. Low ambient humidity impairs barrier function and innate resistance against influenza infection. Proc. Natl. Acad. Sci. U. S. A. 116 (22), 10905–10910.

Lau, E.H.Y., Cowling, B.J., Ho, L.M., Leung, G.M., 2008. Optimizing use of multistream influenza sentinel surveillance data. Emerg. Infect. Dis. 14 (7), 1154–1157.

Lipsitch, M., Viboud, C., 2009. Influenza seasonality: lifting the fog. Proc. Natl. Acad. Sci. U. S. A. 106 (10), 3645–3646.

Lofgren, E., Fefferman, N.H., Naumov, Y.N., Gorski, J., Naumova, E.N., 2007. Influenza seasonality: underlying causes and modeling theories. J. Virol. 81 (11), 5429–5436.

Lowen, A., Palese, P., 2009. Transmission of influenza virus in temperate zones is predominantly by aerosol, in the tropics by contact: a hypothesis. PLoS Curr. 1, RRN1002.

Lowen, A.C., Steel, J., 2014. Roles of humidity and temperature in shaping influenza seasonality. J. Virol. 88 (14), 7692–7695.

Lowen, A.C., Mubareka, S., Steel, J., Palese, P., 2007. Influenza virus transmission is dependent on relative humidity and temperature. PLoS Pathog. 3 (10), 1470–1476.

Lowen, A.C., Steel, J., Mubareka, S., Palese, P., 2008. High temperature (30 degrees C) blocks aerosol but not contact transmission of influenza virus. J. Virol. 82 (11), 5650–5652.

Marr, L.C., Tang, J.W., Van Mullekom, J., Lakdawala, S.S., 2019. Mechanistic insights into the effect of humidity on airborne influenza virus survival, transmission and incidence. J. R. Soc. Interface 16 (150), 20180298.

McDevitt, J., Rudnick, S., First, M., Spengler, J., 2010. Role of absolute humidity in the inactivation of influenza viruses on stainless steel surfaces at elevated temperatures. Appl. Environ. Microbiol. 76 (12), 3943–3947.

Moriyama, M., Ichinohe, T., 2019. High ambient temperature dampens adaptive immune responses to influenza a virus infection. Proc. Natl. Acad. Sci. U. S. A. 116 (8), 3118–3125.

Moriyama, M., Hugentobler, W.J., Iwasaki, A., 2020. Seasonality of respiratory viral infections. Annu. Rev. Virol. 7 (1), 83–101.

Nguyen, J.L., Schwartz, J., Dockery, D.W., 2014. The relationship between indoor and outdoor temperature, apparent temperature, relative humidity, and absolute humidity. Indoor Air 24 (1), 103–112.

Polozov, I.V., Bezrukov, L., Gawrisch, K., Zimmerberg, J., 2008. Progressive ordering with decreasing temperature of the phospholipids of influenza virus. Nat. Chem. Biol. 4 (4), 248–255.

Prussin 2nd, A.J., Schwake, D.O., Lin, K., Gallagher, D.L., Buttling, L., Marr, L.C., 2018. Survival of the enveloped virus Phi6 in droplets as a function of relative humidity, absolute humidity, and temperature. Appl. Environ. Microbiol. 84 (12).

Ryu, S., Ali, S.T., Cowling, B.J., Lau, E.H.Y., 2020. Effects of school holidays on seasonal influenza in South Korea, 2014–2016. J. Infect. Dis. 222 (5), 832–835.

Shaman, J., Kohn, M., 2009. Absolute humidity modulates influenza survival, transmission, and seasonality. Proc. Natl. Acad. Sci. U. S. A. 106 (9), 3243–3248.

Shaman, J., Pitzer, V.E., Viboud, C., Grenfell, B.T., Lipsitch, M., 2010. Absolute humidity and the seasonal onset of influenza in the continental United States. PLoS Biol. 8 (2), e1000316.

Shaman, J., Goldstein, E., Lipsitch, M., 2011. Absolute humidity and pandemic versus epidemic influenza. Am. J. Epidemiol. 173 (2), 127–135.

Tamerius, J., Nelson, M.I., Zhou, S.Z., Viboud, C., Miller, M.A., Alonso, W.J., 2011. Global influenza seasonality: reconciling patterns across temperate and tropical regions. Environ. Health Perspect. 119 (4), 439–445.

Tamerius, J.D., Shaman, J., Alonso, W.J., et al., 2013. Environmental predictors of seasonal influenza epidemics across temperate and tropical climates. PLoS Pathog. 9 (3), e1003194.

Tan, Y., Lam, T.T., Wu, C., et al., 2014. Increasing similarity in the dynamics of influenza in two adjacent subtropical chinese cities following the relaxation of border restrictions. J. Gen. Virol. 95 (Pt 3), 531–538.

Tang, J.W., Lai, F.Y., Nymadawa, P., et al., 2010. Comparison of the incidence of influenza in relation to climate factors during 2000–2007 in five countries. J. Med. Virol. 82 (11), 1958–1965.

te Beest, D.E., van Boven, M., Hooiveld, M., van den Dool, C., Wallinga, J., 2013. Driving factors of influenza transmission in the Netherlands. Am. J. Epidemiol. 178 (9), 1469–1477.

te Beest, D.E., Wallinga, J., Donker, T., van Boven, M., 2013. Estimating the generation interval of influenza a (H1N1) in a range of social settings. Epidemiology 24 (2), 244–250.

Wong, J.Y., Wu, P., Nishiura, H., et al., 2013. Infection fatality risk of the pandemic A (H1N1)2009 virus in Hong Kong. Am. J. Epidemiol. 177 (8), 834–840.

Wu, J.T., Cowling, B.J., Lau, E.H., 2010. School closure and mitigation of pandemic (H1N1) 2009, Hong Kong. Emerg. Infect. Dis. 16 (3), 538–541.

Wu, P., Goldstein, E., Ho, L.M., et al., 2012. Excess mortality associated with influenza a and B virus in Hong Kong, 1998–2009. J. Infect. Dis. 206 (12), 1862–1871.

Wu, P., Presanis, A.M., Bond, H.S., Lau, E.H.Y., Fang, V.J., Cowling, B.J., 2017. A joint analysis of influenza-associated hospitalizations and mortality in Hong Kong, 1998–2013. Sci. Rep. 7 (1), 929.

Xia, Y.C., Gog, J.R., Grenfell, B.T., 2005. Semiparametric estimation of the duration of immunity from infectious disease time series: influenza as a case-study. J. Roy. Stat. Soc. C App. 54, 659–672.

Yang, L., Wong, C.M., Lau, E.H., Chan, K.P., Ou, C.Q., Peiris, J.S., 2008. Synchrony of clinical and laboratory surveillance for influenza in Hong Kong. PLoS One 3 (1), e1399.

Yang, W., Cowling, B.J., Lau, E.H., Shaman, J., 2015. Forecasting influenza epidemics in Hong Kong. PLoS Comput. Biol. 11 (7), e1004383.